Track Fusion with Road Constraints

Chun Yang
Sigtem Technology, Inc.
1343 Parrott Drive
San Mateo, CA 94402
chunyang@sigtem.com

Erik Blasch
Air Force Research Lab/SNAA
2241 Avionics Circle
WPAFB, OH 45433
erik.blasch@wpafb.af.mil

***Abstract*–*This paper is concerned with tracking of ground targets on roads and investigates possible ways to improve target state estimation via fusing a target's track with information about a road along which the target is believed to be traveling. A target track is estimated by a surveillance radar whereas a digital map provides the road network of a region under surveillance. When the information about roads is as accurate as (or even better than) radar measurements, it is desired naturally to incorporate such information (fusion) into target state estimation. In this paper, roads are modeled with analytic functions and its fusion with a target track is cast as linear or nonlinear state constraints in an optimization procedure. The constrained optimization is then solved with the Lagrangian multiplier, leading to a closed-form solution for linear constraints and an iterative solution for nonlinear constraints. Geometric interpretations of the solutions are provided for simple cases. Computer simulation results are presented to illustrate the algorithms.*

Keywords: Track fusion, Road map, State constraints, Lagrangian multiplier, Iterative solution

1. Introduction

With the rapid building up of geographic information system (GIS) including digital road maps (DRM) and digital terrain elevation database (DTED), information about roads becomes more accurate, which is also more up to date and easily accessible. Target tracking is not unfamiliar with road maps. As examples, target tracks are represented by colorful dots and lines blinking along road networks on a large screen, often on top of a topographic or satellite image, in a situation room, in an air traffic control tower, and on a radar operator screen. In these applications, however, target tracks and road networks are merely displayed together with little or no interaction (fusion) in the data processing level.

When the information about roads is as accurate as (or even better than) radar measurements, it is desired naturally to incorporate such information (fusion) into target state estimation. When a vehicle travels off-road or on an unknown road, the state estimation problem is unconstrained. However, when the vehicle is traveling on a known road, be it straight or curved, the state estimation problem can be cast as constrained with the road network information available from digital road/terrain maps. In the past, such constraints are often ignored (or left for the users to perceive it as in the display example mentioned above). The resulting estimates, even obtained with the Kalman filter, cannot be optimal because they do not make full use of this additional information about state constraints.

To use such state constraints, previous attempts can be put into several groups. The first group is to incorporate road information into the state estimation process [5, 6, 9, 11]. The second group is to treat state constraints as perfect (pseudo) measurements. For a road segment, its analytic model not only constrains the target position but also the direction of the target's velocity vector. Indeed, the target velocity vector is closely aligned with the road orientation for a linear segment and with the tangent vector at the target position for a nonlinear segment. Furthermore, an estimate of centripetal acceleration can be obtained given the curvature and the target speed.

In the third group, an unconstrained Kalman filter solution is first obtained and then the unconstrained state estimate is projected onto the constrained surface [10]. This technique can also be viewed as post-processing (estimation or updating) correction [11] or track to road fusion referred to as in this paper. In conventional track fusion, two or more tracks are available, each consisting of an estimate of the underlying track with its estimation error covariance. The fused track is typically found that minimizes the sum of covariance–weighted state errors squared [3, 4]. In contrast to this conventional track fusion that operates on individual state values (points), track fusion with road involves a state value (a point) and a subset of state values (an interval). In this paper, roads are modeled with analytic functions and its fusion with a target track is therefore formulated as linear or nonlinear state constraints in an optimization procedure.

Report Documentation Page

Form Approved
OMB No. 0704-0188

1. REPORT DATE	2. REPORT TYPE	3. DATES COVERED
JUL 2007		**00-00-2007 to 00-00-2007**

4. TITLE AND SUBTITLE	5a. CONTRACT NUMBER
Track Fusion with Road Constraints	5b. GRANT NUMBER
	5c. PROGRAM ELEMENT NUMBER
6. AUTHOR(S)	5d. PROJECT NUMBER
	5e. TASK NUMBER
	5f. WORK UNIT NUMBER
7. PERFORMING ORGANIZATION NAME(S) AND ADDRESS(ES) **Air Force Research Lab/SNAA,2241 Avionics Circle,Wright Patterson AFB,OH,45433**	8. PERFORMING ORGANIZATION REPORT NUMBER
9. SPONSORING/MONITORING AGENCY NAME(S) AND ADDRESS(ES)	10. SPONSOR/MONITOR'S ACRONYM(S)
	11. SPONSOR/MONITOR'S REPORT NUMBER(S)

12. DISTRIBUTION/AVAILABILITY STATEMENT
Approved for public release; distribution unlimited

13. SUPPLEMENTARY NOTES
10th International Conference on Information Fusion, 9-12 July 2007, Quebec, Canada.

14. ABSTRACT
see report

15. SUBJECT TERMS

16. SECURITY CLASSIFICATION OF:			17. LIMITATION OF ABSTRACT	18. NUMBER OF PAGES	19a. NAME OF RESPONSIBLE PERSON
a. REPORT **unclassified**	b. ABSTRACT **unclassified**	c. THIS PAGE **unclassified**	**Same as Report (SAR)**	**8**	

In this paper, the constrained optimization is solved with the Lagrangian multiplier, leading to a closed-form solution for linear constraints and an iterative solution for nonlinear constraints. In the latter case, we present a method that allows for the use of second-order nonlinear state constraints exactly. The method can provide better approximation to higher order nonlinearities. The new method is based on a computational algorithm that iteratively finds the Lagrangian multiplier. The use of a second-order constraint vs. linearization is a tradeoff between reducing approximation errors to higher-order nonlinearities and keeping the problem computationally tractable.

Although the main results are restricted to state equality constraints, it can be extended to inequality constraints. According to [10], the inequality constraints can be checked at each time step of filtering. If the inequality constraints are satisfied at a given time step, no action is taken since the inequality constrained problem is solved. If the inequality constraints are not satisfied at a given time step, then the constrained solution is applied to enforce the constraints.

2. Track Fusion with Linear Road Segment

When a road segment is straight, it can be modeled as a linear state constraint. In this section, we first summarize the results for linearly constrained state estimation [10] as an approach to track fusion with linear road segments. We then show that this linearly constrained state estimation is equivalent to use of constraints as measurements in state update. Finally, we provide a simple geometric interpretation of the linearly constrained state estimation for track to road fusion.

Consider a linear time-invariant discrete-time dynamic system together with its measurement as

$$\underline{x}_{k+1} = A\underline{x}_k + B\underline{u}_k + \underline{w}_k \tag{1a}$$

$$\underline{y}_k = C\underline{x}_k + \underline{v}_k \tag{1b}$$

where the underscore indicates a vector quantity, the subscript k is the time index, $\underline{x}$ is the state vector, $\underline{u}$ is a known input, $\underline{y}$ is the measurement, and $\underline{w}$ and $\underline{v}$ are state and measurement noise processes, respectively. It is implied that all vectors and matrices have compatible dimensions, which are omitted for simplicity.

The goal is to find an estimate denoted by $\hat{\underline{x}}_k$ of $\underline{x}_k$ given the measurements up to time k denoted by $Y_k = \{\underline{y}_0, \ldots, \underline{y}_k\}$. Under the assumptions that the state and measurement noises are uncorrelated zero-mean white Gaussian with $\underline{w} \sim \mathcal{N}\{0, Q\}$ and $\underline{v} \sim \mathcal{N}\{0, R\}$ where Q and R are positive semi-definite covariance matrices, the Kalman filter provides an optimal estimator in the form of $\hat{\underline{x}}_k = E\{\underline{x}_k \mid Y_k\}$ [2]. Starting from an initial estimate $\hat{\underline{x}}_0 = E\{\underline{x}_0\}$ and its estimation error covariance matrix $P_0 = E\{(\underline{x}_0 - \hat{\underline{x}}_0)(\underline{x}_0 - \hat{\underline{x}}_0)^T\}$ where the superscript T stands for matrix transpose, the Kalman filter equations specify the propagation of $\hat{\underline{x}}_k$ and P_k over time and the update of $\hat{\underline{x}}_k$ and P_k by measurement $\underline{y}_k$ as

$$\bar{\underline{x}}_{k+1} = A\hat{\underline{x}}_k + B\underline{u}_k \tag{2a}$$

$$\bar{P}_{k+1} = AP_kA^T + Q \tag{2b}$$

$$\hat{\underline{x}}_{k+1} = \bar{\underline{x}}_{k+1} + K_{k+1}(\underline{y}_{k+1} - C\bar{\underline{x}}_{k+1}) \tag{2c}$$

$$P_{k+1} = (I - K_{k+1}C)\bar{P}_{k+1} \tag{2d}$$

$$K_{k+1} = \bar{P}_{k+1}C^T(CP_kC^T + R)^{-1} \tag{2e}$$

where $\bar{\underline{x}}_{k+1}$ and $\bar{P}_{k+1}$ are the predicted state and prediction error covariance, respectively.

Now in addition to the dynamic system of (1), we are given the linear state constraint equation

$$D\underline{x}_k = \underline{d} \tag{3}$$

where D is a known constant matrix of full rank, $\underline{d}$ is a known vector, and the number of rows in D is the number of constraints, which is assumed to be less than the number of states. If D is a square matrix, the state is fully constrained and can thus be solved by inverting (3). Although no time index is given to D and $\underline{d}$ in (3), it is implied that they can be time-dependent, leading to piecewise linear constraints.

The constrained Kalman filter according to [10] is constructed by directly projecting the unconstrained state estimate $\hat{\underline{x}}_k$ onto the constrained surface $S = \{\underline{x}: D\underline{x} = \underline{d}\}$. It is formulated as the solution to the problem

$$\breve{\underline{x}} = \arg\min_{\underline{x}\in S}(\underline{x} - \hat{\underline{x}})^T W(\underline{x} - \hat{\underline{x}}) \tag{4}$$

where W is a symmetric positive definite weighting matrix.

Derived using the Lagrangian multiplier technique [16], the solution to the constrained optimization in (4) is given by

$$\breve{\underline{x}} = \hat{\underline{x}} - W^{-1}D^T(DW^{-1}D^T)^{-1}(D\hat{\underline{x}} - \underline{d}) \tag{5}$$

As described above, the linear constrained estimator (5) can be obtained by different methods. It is shown in this section that it is also equivalent to the solution where the linear state constraints are considered as perfect (pseudo) measurements.

For the linear time-invariant discrete-time dynamic system (1a) and its measurement (1b), consider the linear state constraint (3) as another measurement to the system, which can be used to perform the filter

measurement update (2c) and (2d) right after (1b) without the filter time propagation (2a) and (2b) (i.e., stay the same). To apply (2), we identify the following equivalence:

$A = I, B = 0; Q = 0$ (6a)

$C = D, R = 0, \underline{y}_k = \underline{d}$ (6b)

Given the unconstrained solution $(\hat{\underline{x}}_k, P_k)$, the prediction step is given by (2a) and (2b):

$$\bar{\underline{x}}_{k+1} = \hat{\underline{x}}_k \quad (7a)$$

$$\bar{P}_{k+1} = P_k \quad (7b)$$

The Kalman filter gain is given by:

$$K_{k+1} = P_k D^T (DP_k D^T)^{-1} \quad (8)$$

The updated state and error covariance becomes:

$$\hat{\underline{x}}_{k+1} = \hat{\underline{x}}_k + P_k D^T (DP_k D^T)^{-1} (\underline{d} - D\hat{\underline{x}}_k) \quad (9a)$$

$$P_{k+1} = P_k - P_k D^T (DP_k D^T)^{-1} DP_k \quad (9b)$$

If we choose $W = P_k^{-1}$, (9a) becomes

$$\hat{\underline{x}}_{k+1} = \hat{\underline{x}}_k + W^{-1} D^T (DW^{-1} D^T)^{-1} (\underline{d} - D\hat{\underline{x}}_k) \quad (10a)$$

$$= \hat{\underline{x}}_k - W^{-1} D^T (DW^{-1} D^T)^{-1} (D\hat{\underline{x}}_k - \underline{d}) \quad (10b)$$

which is exactly the same as the solution given by (5).

Assume that the state dimension is n and the number of linear constraints is $m < n$. For $\underline{x} \in R^n$, the constraint surface $S = \{\underline{x}: D\underline{x} = \underline{d}\}$ is not a subspace simply because for $\underline{d} \neq 0$, the null vector is not inside S.

To construct a subspace, first find an arbitrary point $\underline{x}_0 \in S$ and then define $\underline{\xi} = \underline{x} - \underline{x}_0$. This is equivalent to shifting the origin of the coordinates to $\underline{x}_0$, thus performing an affine transformation denoted by T. For all $\underline{x} \in S$, the corresponding shifted vector $\underline{\xi}$ has the following property:

$$D\underline{\xi} = D(\underline{x} - \underline{x}_0) = D\underline{x} - D\underline{x}_0 = \underline{d} - \underline{d} = 0 \quad (11)$$

In other words, the constraint surface after the affine transformation T becomes a subspace, denoted by $\mathcal{L} = TS = \{\underline{\xi}: D\underline{\xi} = 0\}$, which has a dimension n-m. The affine transformation is illustrated in Fig. 1.

We are now to express $\mathcal{L}$. But first, the row vectors of D can be expressed as:

$$D^T = [\underline{d}_1 \quad \underline{d}_2 \quad \cdots \quad \underline{d}_m] \quad (12)$$

Since D is of full rank by assumption, the row vectors of D can be used as the non-orthogonal bases for a subspace denoted by $\mathcal{D} = \text{span}\{\underline{d}_1, \underline{d}_2, \ldots, \underline{d}_m\}$. In light of (11) and by definition of $\mathcal{L}$, it is easy to see that $\mathcal{D}$ is an orthogonal complement of $\mathcal{L}$, that is, $\mathcal{D} \perp \mathcal{L}$ and $\mathcal{D} \oplus \mathcal{L} = R^n$.

For $\underline{\delta} \in \mathcal{D}$, it can be written as:

$$\underline{\delta} = \sum_{i=1}^{m} c_i \underline{d}_i = [\underline{d}_1 \quad \underline{d}_2 \quad \cdots \quad \underline{d}_m] \begin{bmatrix} c_1 \\ c_2 \\ \vdots \\ c_m \end{bmatrix} = D^T \underline{c} \quad (13)$$

Then for $\underline{\xi} \in \mathcal{L}$, we have

$$< \underline{\delta}, \underline{\xi} > = < D^T \underline{c}, \underline{\xi} > = \underline{\delta}^T \underline{\xi} = \underline{c}^T D\underline{\xi} = 0 \quad (14)$$

where $<\underline{a}, \underline{b}> = \underline{a}^T \underline{b}$ is the inner product defined on R^n.

By the principle of orthogonality, an arbitrary vector $\underline{\xi}$ can be decomposed into its projections onto the orthogonal complements $\mathcal{D}$ and $\mathcal{L}$, denoted by $\underline{\xi}_D$ and $\underline{\xi}_L$, respectively, as

$$\underline{\xi} = \underline{\xi}_D + \underline{\xi}_L \quad (15)$$

Adding $\underline{x}_0$ to both sides of (15), we can express the vectors in the original coordinates as:

$$\underline{x} = \underline{\xi} + \underline{x}_0 = \underline{\xi}_D + \underline{\xi}_L + \underline{x}_0 = \underline{\xi}_D + \underline{x}^* \quad (16)$$

The projection of the arbitrary vector on the constraint subspace $\mathcal{L}$ and the constraint surface S can be obtained, respectively, as:

$$\underline{\xi}_L = \underline{\xi} - \underline{\xi}_D \quad (17a)$$

$$\underline{x}^* = \underline{x} - \underline{\xi}_D \quad (17b)$$

To obtain $\underline{\xi}_D$, express it as a linear combination of the non-orthogonal bases of D^T with the coefficient vector $\underline{c}$ as:

$$\underline{\xi}_D = \sum_{i=1}^{m} c_i \underline{d}_i = [\underline{d}_1 \quad \underline{d}_2 \quad \cdots \quad \underline{d}_m] \begin{bmatrix} c_1 \\ c_2 \\ \vdots \\ c_m \end{bmatrix} = D^T \underline{c} \quad (18)$$

Again, by the principle of orthogonality, the projection error vector $\underline{\xi} - \underline{\xi}_D$ is orthogonal to $\mathcal{D}$, *i.e.*, each an every basis of it:

$$< \underline{\xi} - \underline{\xi}_D, \underline{d}_i > = < \underline{\xi} - D^T \underline{c}, \underline{d}_i > = \underline{d}_i^T (\underline{\xi} - D^T c) = 0, \quad i = 1, \ldots, m \quad (19)$$

Stacking these orthogonality conditions, we obtain

$$\begin{bmatrix} \underline{d}_1^T \\ \underline{d}_2^T \\ \vdots \\ \underline{d}_m^T \end{bmatrix} (\underline{\xi} - D^T \underline{c}) = 0 \quad \text{or } D(\underline{\xi} - D^T \underline{c}) = 0 \quad (20)$$

Since DD^T is an $m \times m$ matrix and invertible, the coefficient vector can be obtained as:

$$\underline{c} = (DD^T)^{-1} D\underline{\xi} \quad (21)$$

Bringing (21) back to (18) gives the projection vector as:

$$\underline{\xi}_D = D^T(DD^T)^{-1}D\underline{\xi} = P\underline{\xi} \quad (22)$$

where $P = D^T(DD^T)^{-1}D$ is usually referred to as the projection matrix onto $\mathcal{D}$ and (I-P) is the projection matrix onto $\mathcal{L}$.

Bringing (22) back to (17) gives

$$\underline{\xi}_L = \underline{\xi} - P\underline{\xi} = (I-P)\underline{\xi} \quad (23a)$$

$$\underline{x}^* = \underline{x} - P\underline{\xi} = \underline{x} - P(\underline{x} - \underline{x}_0) \quad (23b)$$

Bringing the expression for P into (23b) gives

$$\begin{aligned}\underline{x}^* &= \underline{x} - D^T(DD^T)^{-1}D(\underline{x} - \underline{x}_0)\\ &= \underline{x} - D^T(DD^T)^{-1}(D\underline{x} - D\underline{x}_0)\\ &= \underline{x} - D^T(DD^T)^{-1}(D\underline{x} - \underline{d}) \quad (24)\end{aligned}$$

where $D\underline{x}_0 = \underline{d}$ is used to arrive at the last equation because of $\underline{x}_0 \in S$.

(24) is exactly the same as (5) when $W = I$. This offers a geometrical interpretation that the linear constrained estimation is the orthogonal projection of the unconstrained estimate onto the constrained surface. It provides a theoretical justification of the intuitive practice of finding a point along the road that is of the shortest distance.

The theory still holds for $W \neq I$. The results presented in this paper complement [10], providing an interesting geometrical interpretation to the linear constrained estimation by estimate projection.

3. Track Fusion with Nonlinear Road Segments

When a road segment is curved, it can be modeled as a nonlinear state constraint. In this section, we first analyze the linearizing approach and the associated constraint approximation error. We then present an iterative solution to a second order state constraint. Finally, we offer a geometric interpretation of a solution under a circular constraint and a simple approach to a more general second order state constraint.

To deal with nonlinearity, a simple approach is to project the unconstrained state estimate onto linearized state constraints. Once the constraints are linearized, the results presented in the previous section for linear cases can be applied. However, linearization introduces constraint approximation error, which is a function of the nonlinearity and, more importantly, of the point around which the linearization takes place. This may lead to an undesired divergence problem as analyzed below.

Fig. 2 illustrates this linearization process and identifies possible errors associated with linear approximation of a nonlinear state constraint. As shown, the previous constrained state estimate $\breve{\underline{x}}^-$ lies somewhere on the constrained surface but is away from the true state $\underline{x}$. The projection of the unconstrained state estimate $\hat{\underline{x}}$ onto the approximate linear state constraint produces the current constrained state estimate $\breve{\underline{x}}^+$, which is however subject to the constraint approximation error. Clearly, the further away is $\breve{\underline{x}}^-$ from $\underline{x}$, the larger is the approximation-introduced error. More critically, such an approximately linear constrained estimate may not satisfy the original nonlinear constraint. It is therefore desired to reduce this approximation-introduced error by including higher-order terms while keeping the problem computationally tractable. One possible approach is presented in the next section.

Naturally formed roads tend to have more bends and turns of irregular shapes (high nonlinearity). Even highways have to follow terrain contours when crossing mountains. Locally, however, it suffices to represent a curved road segment by a second-order state constraint function as

$$\begin{aligned}f(\underline{x}) &= \begin{bmatrix}\underline{x}^T & 1\end{bmatrix}\begin{bmatrix}M & \underline{m}\\ \underline{m}^T & m_0\end{bmatrix}\begin{bmatrix}\underline{x}\\ 1\end{bmatrix}\\ &= \underline{x}^T M\underline{x} + \underline{m}^T\underline{x} + \underline{x}^T\underline{m} + m_0 = 0 \quad (26)\end{aligned}$$

which can be viewed as a second-order approximation to an arbitrary nonlinearity in a digital terrain map.

Similar to (4), we can formulate the projection of an unconstrained state estimation onto a nonlinear constraint surface as the constrained least-square optimization problem

$$\hat{\underline{x}} = \arg\min_{\underline{x}}(\underline{z} - H\underline{x})^T(\underline{z} - H\underline{x}) \quad (27a)$$

subject to $f(\underline{x}) = 0$ (27b)

If we let $W = H^TH$ and $z = H\hat{x}$, the formulation in (27) becomes the same as in (4). In a sense, (27) is a more general formulation because it can also be interpreted as a nonlinear constrained measurement update or a projection in the predicted measurement domain.

The solution to the constrained optimization (27) can be obtained again using the Lagrangian multiplier technique as [12]

$$\hat{\underline{x}} = G^{-1}V(I + \lambda\Sigma^T\Sigma)^{-1}\underline{e}(\lambda) \quad (28a)$$

$$q(\lambda) = \sum_i \frac{e_i^2(\lambda)\sigma_i^2}{(1+\lambda\sigma_i^2)^2} + 2\sum_i \frac{e_i(\lambda)t_j}{1+\lambda\sigma_i^2} + m_0 = 0 \quad (28b)$$

where G is an upper right diagonal matrix resulting from the Cholesky factorization of $W = H^TH$, V, an orthonormal matrix, and Σ, a diagonal matrix with its diagonal elements denoted by σ_i, are obtained from the singular value decomposition of the matrix LG^{-1}, and

$\underline{e}(\lambda) = [\ldots\ e_i(\lambda), \ldots]^T = V^T(G^T)^{-1}(H^T\underline{z} - \lambda\underline{m})$ (29c)

$\underline{t} = [\ldots\ t_i\ \ldots]^T = V^T(G^T)^{-1}\underline{m}$ (29d)

As a nonlinear equation in λ, it is difficult to find a closed-form solution in general for the nonlinear equation $q(\lambda) = 0$ in (28b). Numerical root-finding algorithms may be used instead. For example, the Newton's method is used below. Denote the derivative of $q(\lambda)$ with respect to λ as $\dot{q}(\lambda)$. Then the iterative solution for λ is given by

$$\lambda_{k+1} = \lambda_k - \frac{q(\lambda_k)}{\dot{q}(\lambda_k)}, \text{ starting with } \lambda_0 = 0 \quad (30)$$

Now consider the special case where $W = H^TH$, $z = H\underline{\hat{x}}$, and $\underline{m} = 0$, that is, a quadratic constraint on the state. Under these conditions, $\underline{t} = 0$ and $\underline{e}$ is no longer a function of λ so its derivative relative to λ vanishes. The quadratic constrained solution is then given by

$$\underline{\breve{x}} = (W+\lambda M)^{-1}W\underline{\hat{x}} \quad (31a)$$

where the Lagrangian multiplier λ is obtained iteratively as in (30) with the corresponding $q(\lambda)$ and $\dot{q}(\lambda)$ given by

$$q(\lambda) = \sum_i \frac{e_i^2\sigma_i^2}{(1+\lambda\sigma_i^2)^2} + m_0 = 0 \quad (31b)$$

$$\dot{q}(\lambda) = -2\sum_i \frac{e_i^2\sigma_i^4}{(1+\lambda\sigma_i^2)^3} \quad (31c)$$

The solution of (31) is also called the constrained least squares [8: pp 765-766], which was previously applied for the joint estimation and calibration [13]. Similar techniques have been used for the design of filters for radar applications [1] and in robust minimum variance beamforming [7]. When $M = 0$, the constraint in (26) degenerates to a linear one. The constrained solution is still valid. However, the iterative solution for finding λ is no longer applicable but a closed-form solution is available instead as given in (5).

Consider a simple example where a target travels along a circle. For this case, in fact, a closed-form solution can be derived. Assume that $W = I_2$, $M = I_2$, $\underline{m} = 0$, and $m_0 = -r^2$. The nonlinear constraint can be equivalently written as:

$$\underline{x}^T\underline{x} = r^2 \quad (32)$$

The quadratic constrained estimate given in (31a) becomes:

$$\underline{\breve{x}} = (W + \lambda M)^{-1}W\underline{\hat{x}} = (1+\lambda)^{-1}\underline{\hat{x}} \quad (33)$$

Bringing (35) back to (34) gives:

$$\underline{\breve{x}}^T\underline{\breve{x}} = \left(\frac{\hat{\underline{x}}}{1+\lambda}\right)^T\frac{\hat{\underline{x}}}{1+\lambda} = r^2 \quad (34)$$

The solution for λ is:

$$\lambda = \frac{\sqrt{\hat{\underline{x}}^T\hat{\underline{x}}}}{r} - 1 = \frac{\|\hat{\underline{x}}\|_2}{r} - 1 \quad (35)$$

where $\|\cdot\|_2$ stands for the 2-norm of the vector.

Bringing the solution for λ in (35) back to (33) gives:

$$\underline{\breve{x}} = r\frac{\hat{\underline{x}}}{\|\hat{\underline{x}}\|_2} \quad (36)$$

This indicates that for this particular case with a circular constraint, the constraining results in normalization. This further suggests a simple solution for some practical applications. When a target is traveling along a circular path (or approximately so), one can first find the equivalent center of the circle around which to establish a new coordinate system. Then express the unconstrained solution in the new coordinate and normalize it as the constrained solution. Finally convert it back to the original coordinates.

4. Simulation Results

In this simulation example, a ground vehicle is assumed to travel along a circular road segment as shown in Fig. 2. The turn center is chosen as the origin of the *x*-*y* coordinates and the turn radius is r = 100 m. The target maintains a constant turn rate of 5.7 deg/s with an equivalent linear speed of 10 m/s. The initial state is

$$\underline{x}_{k=0} = [x \quad \dot{x} \quad y \quad \dot{y}]^T = [100\text{ m}, 0\text{ m/s}, 0\text{ m } 10\text{ m/s}]^T \quad (37)$$

The vehicle is tracked by a radar sensor with a sampling interval of T = 1 s. The sensor provides position measurements of the vehicle as

$$\underline{y}_k = \begin{bmatrix} 1 & 0 & 0 & 0 \\ 0 & 0 & 1 & 0 \end{bmatrix}\underline{x}_k + \underline{v}_k \quad (38)$$

where the measurement error $\underline{v} \sim \mathcal{N}(\underline{0}, R)$ is a zero-mean Gaussian noise, independent in the *x*- and *y*-axis. The covariance matrix $R = \text{diag}([\sigma_{rx}^2\ \ \sigma_{ry}^2])$ uses the particular values of $\sigma_{rx} = \sigma_{ry} = 7$ m in the simulation.

The radar implements a simple tracker based on the following discrete-time second-order kinematic model

$$\underline{x}_{k+1} = \begin{bmatrix} 1 & T & 0 & 0 \\ 0 & 1 & 0 & 0 \\ 0 & 0 & 1 & T \\ 0 & 0 & 0 & 1 \end{bmatrix}\underline{x}_k + \begin{bmatrix} \frac{1}{2}T^2 & 0 \\ T & 0 \\ 0 & \frac{1}{2}T^2 \\ 0 & T \end{bmatrix}\underline{w}_k \quad (39)$$

where the process noise $\underline{w} \sim \mathcal{N}(\underline{0}, Q)$ is also a zero-mean Gaussian noise, independent of the measurement noise $\underline{v}$. The covariance matrix $Q = \text{diag}([\sigma_{\ddot{x}}^2\ \ \sigma_{\ddot{y}}^2])$ uses the particular values of $\sigma_{\ddot{x}} = \sigma_{\ddot{y}} = 0.32$ m/s^2 in the simulation.

When represented in a Cartesian coordinate system, a target traveling along a curved road is certainly subject to acceleration in both the *x*- and *y*-axis. However, no effect is made in this simulation to optimize the tracker for maneuver but merely to select *Q* and the initial conditions so as to focus on constraining the estimates. The initial state is selected to be the same as the true state, i.e., $\underline{\hat{x}}_0 = \underline{x}_0$ and the initial estimation error covariance is selected to be

$P_0 = \text{diag}([5^2 \;\; 1^2 \;\; 5^2 \;\; 1^2])$

Fig. 3 shows sample trajectories of the linear constrained Kalman filter. There are 5 curves and 2 series of data points in the figure. The true state is represented by a series of dots (·) at consecutive sampling instants, which is plotted on the solid line being the road segment. The corresponding measurements are a series of circles (o).

The estimates of the unconstrained Kalman filter are shown as the connected triangles (Δ) whereas those of linearly constrained Kalman filters are shown as the connected crosses (x), stars (*), and pluses (+) for three linear approximations of the nonlinear constraint of curved road, respectively.

In the first approximation (the line with cross x labeled "linear constraint 1"), a single linearizing point at $\theta_1 = 10^o$ is chosen to cover the entire curved road, where θ is the angle made relative to the x-axis, positive in the counter-clock direction. The linearized state constraint at θ_1 can be written as

$$\begin{bmatrix} \cos\theta_1 & 0 & \sin\theta_1 & 0 \\ 0 & \cos\theta_1 & 0 & \sin\theta_1 \end{bmatrix} \underline{x} = \begin{bmatrix} r \\ 0 \end{bmatrix} \qquad (40)$$

Although all estimates are faithfully projected by the constrained filter onto this linear constraint, tangential to the curve at the linearizing point, it runs away from the true trajectory and the resulting errors continue to grow. The apparent divergence is caused by the choice of linearization.

In the second approximation (the line with star * labeled "linear constraint 2"), two linearizing points at $\theta_1 = 15^o$ and $\theta_2 = 80^o$ are chosen to cover the curved road with two linear segments. The switching point from one linear segment to the other in this case is at $\theta = 45^o$. As shown, the estimates are projected onto one of the two linear segments. Except near the corner where the two linear approximations intersect (which is far away from both linearizing points), the linear constrained estimates typically outperform the unconstrained estimates (closer to the true state). This is better illustrated in Fig. 4 where the upper plot is for the absolute position error in *x* while the lower plot is for the absolute position error in *y*, both plotted as a function of time.

Still with two linearizing points and the same switching point at $\theta = 45^o$, the third approximation (the line with star + labeled "linear constraint 3") adjusts linearizing points to $\theta_1 = 20^o$ and $\theta_2 = 70^o$. A better overall performance is achieved as shown in Fig. 4.

It is clear from Fig. 3 that a nonlinear constraint can be approximated with linear constraints in a piecewise fashion. By judicious selection of the number of linear segments and their placement (i.e., the point around which to linearize), a reasonably good performance can be expected. In the limit, a nonlinear function is represented by a piecewise function composed of an infinite number of linear segments. This naturally leads to the use of nonlinear constraints. (42)

Fig. 5 shows sample trajectories of the nonlinear constrained Kalman filter. There are 2 curves and 4 series of data points in the figure. The true state is still represented by a series of dots (·) at the sampling instants, which is plotted on the solid line of road segment. The corresponding measurements are again a series of circles (o). The unconstrained Kalman filter is shown as the connected crosses (x) whereas the estimates of nonlinearly constrained Kalman filters are shown as a series of connected pluses (+) and stars (*) for two implementations, respectively.

The first implementation (the series of pluses +) only applies the nonlinear constraint to the position estimate whereas the second implementation (the series of stars *) applies constraints to both the position and velocity estimates. In fact, we encounter a hybrid (mixed) linear and nonlinear state constraint situation. The constrained position estimate is given by (31) for the quadratic case (equivalent to either (36) for a circular road). Since the velocity direction is along the tangent of the road curve, the constrained velocity estimate is obtained by the following projection

$$\underline{\hat{v}}_{constrained} = (\underline{\hat{v}}^T_{unconstrained}\,\underline{\mu})\underline{\mu} \qquad (41)$$

where $\underline{\hat{v}} = [\hat{\dot{x}} \;\; \hat{\dot{y}}]^T$ is the estimated velocity vector and $\underline{\mu} = [-sin\theta \;\; cos\theta]^T$ is the constrained unit direction vector associated with the constrained position at $\theta = \tan^{-1}(\hat{y}/\hat{x})$.

For simplicity, the unconstrained estimation error covariance is not modified in the present simulation after the constrained estimate is obtained using the projection algorithms in (31) and (41). The implementation is therefore pessimistic (suboptimal) in the sense that it does not take into account the reduction in the estimation error covariance brought in by constraining. One consequence of this simplification is more volatile state estimates. To quantify this effect, one approach is to project the unconstrained probability density function (i.e., a normal distribution with

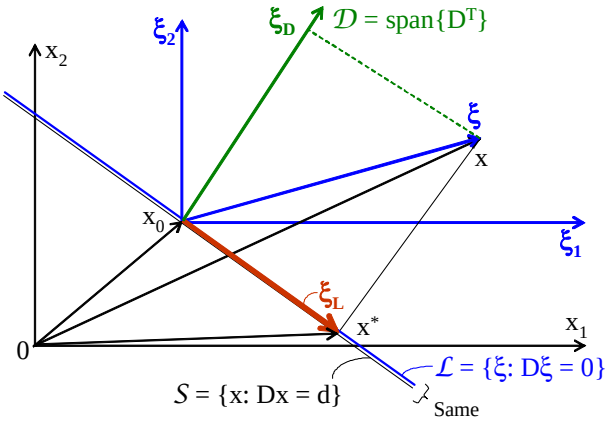

Fig. 1. Geometrical Interpretation of Linear Constrained Solution

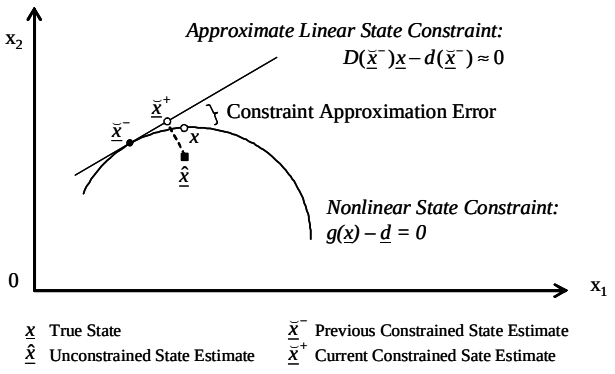

Fig. 2. Errors in Linear Approximation of Nonlinear State Constraints

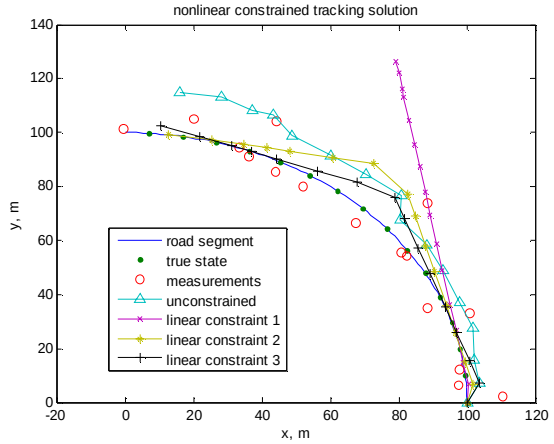

Fig. 3. Sample Trajectories for Linear Constrained Kalman Filter

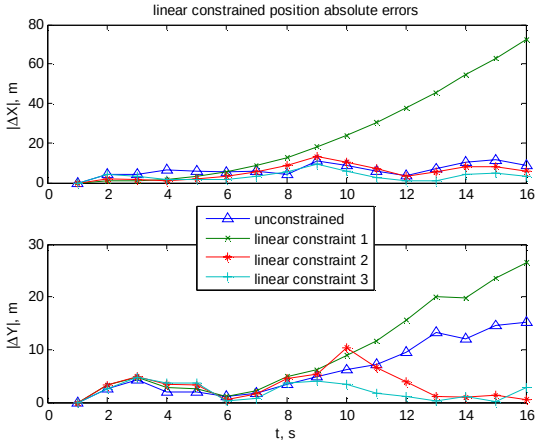

Fig. 4. Linear Constrained Position Errors vs. Time

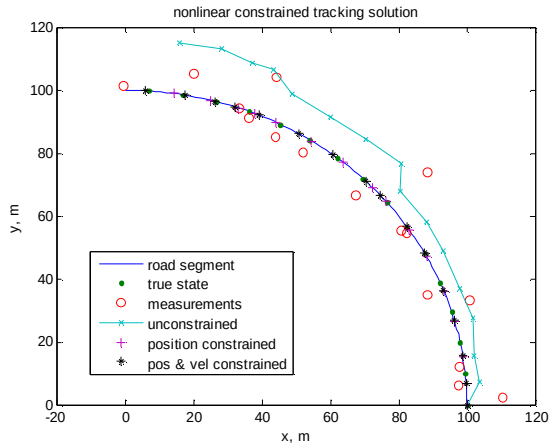

Fig. 5. Sample Trajectories for Nonlinear Constrained Kalman Filter

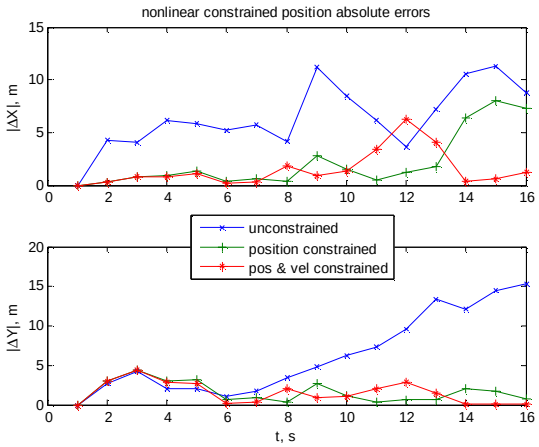

Fig. 6. Nonlinear Constrained Position Errors vs. Time

support on the whole state space) onto the nonlinear constraint. Statistics can then be calculated from the constrained probability density function with the constraint as its support. Again, the resulting error ellipse represented by the covariance matrix is only an approximation to the second order.

As shown in Fig. 5, both the nonlinear constrained estimates fall onto the road as expected. Overall the position and velocity constrained estimates are better (closer to the true state) than the position-only constrained estimates. This is illustrated in Fig. 6 where the upper plot is for the absolute position error in *x* while the lower plot is for the absolute position error in *y*.

A Monte Carlo simulation is used to generate the RMS errors of state estimation. The results are based on a total of 100 runs across 16 updates and summarized in Table 1. The performance improvement of the nonlinear constrained filter over the linearized constrained filter is demonstrated.

Table 1. RMS Estimation Errors

Estimators	RMS Estimation Error	
	Position (m)	Velocity (m/s)
Unconstrained	8.3663	4.2640
Best Linear Constrained	5.5386	2.5466
Nonlinear Constrained	1.8056	0.4252

5. Conclusions

In this paper, we presented an approach to incorporating road information into target tracking via track to road fusion. In this approach, road segments were modeled with analytic functions and their fusion with a target track was cast as a linearly or nonlinearly state constrained optimization procedure. With the Lagrangian multiplier, a closed-form solution was found for linear constraints and an iterative solution for nonlinear constraints. Geometric interpretations of the solutions were provided for simple cases. Computer simulation results demonstrate the performance of the algorithms.

Future work includes both algorithms development and practical applications. It is of interest to extend the iterative method presented in the paper for second-order nonlinear state constraints to other types of nonlinear constraints of practical significance and to search for more efficient root-finding algorithms to solve for the Lagrangian multiplier. Similarly, the simple fusion of a single track to a single road as presented in this paper is being extended to multiple targets moving along closely-spaced road networks with intersections and by-passes. In this case, the fusion (or constraining) can take place in the measurement level as well as in the track level, involving road constrained data association (RCDA). Results will be reported in future papers.

References

[1] Abromovich, Y.I. and Sverdlik, M.B., Synthesis of a Filter Response Which Maximizes the Signal to Noise Ratio under Additional Quadratic Constraints, *Radio Eng. and Electron. Phys.*, **5** (Nov. 1970).

[2] Anderson, B. and Moore, J., *Optimal Filtering*, Englewood Cliffs, NJ: Prentice Hall, 1979.

[3] Bar-Shalom, Y. and Li, X.R., *Multitarget-Multisensor Tracking: Principles and Techniques*, Storrs, CT: YBS Publishing, 1995.

[4] Blackman, S. and R. Popoli, *Design and Analysis of Modern Tracking System*, Boston, MA: Artrch House, 1999.

[5] Kirubarajan, T., Bar-Shalom, Y., Pattipati, K.R., and Kadar, I., Ground Target Tracking with Variable Structure IMM Estimator, *IEEE Trans. On Aerospace and Electronic Systems*, **36** (Jan. 2002).

[6] Ko, S. and Bitmead, R., State Estimation for Linear Systems with State Equality Constraints, *Automatica*, (2005).

[7] Lorenz, R.G. and Boyd, S.P., Robust Minimum Variance Beamforming, In *Robust Adaptive Beamforming*, J. Li and P. Stoica (Eds.). Hoboken, NJ: Wiley-Interscience, 2006.

[8] Moon, T.K. and Stirling, W.C., *Mathematical Methods and Algorithms for Signal Processing*, Upper Saddle River, NJ: Prentice Hall, 2000.

[9] Ristic, B., Arullampalam, S. and Gordon, N., *Beyond the Kalman Filter – Particle Filters for Tracking Applications*, Boston, MA: Artech House, 2004.

[10] Simon, D. and Chia, T.L., Kalman Filtering with State Equality Constraints, *IEEE Trans. On Aerospace and Electronic Systems*, **38** (Jan. 2002).

[11] Yang, C., Bakich, M., and Blasch, E., Nonlinear Constrained Tracking of Targets on Roads, In *Proc. of the 8th International Conf. on Information Fusion*, Philadelphia, PA, July 2005, A8-3 (1-8).

[12] Yang, C. and Blasch, E., Kalman Filtering with Nonlinear State Constraints, In *Proc. of the 9th International Conf. on Information Fusion*, Florence, Italy, July 2006.

[13] Yang, C. and Lin, D.M., Constrained Optimization for Joint Estimation of Channel Biases and Angles of Arrival for Small GPS Antenna Arrays, In *Proc. of the 60th Annual Meeting of the Institute of Navigation*, Dayton, OH, June 2004.